Asian Journal of Chemistry; Vol. 24, No. 1 (2012), 371-376

ASIAN JOURNAL OF CHEMISTRY

www.asianjournalofchemistry.co.in

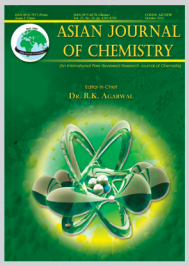

Synthesis and Characterization of Graphene-Based Nanosheets *via* Chemical Reduction of Expanded Graphite Oxide

FENG-JUN ZHANG[1,2], WON-KWEON JANG[3] and WON-CHUN OH[2,*]

[1]Anhui Key Laboratory of Advanced Building Materials, Anhui University of Architecture, Hefei 230022, Anhui Province, P.R. China
[2]Department of Advanced Materials & Science Engineering, Hanseo University, Seosan-si, Chungnam-do 356-706, South Korea
[3]Division of Electronic, Computer and Communication Engineering, Hanseo University, Seosan-si, Chungnam-do 356-706, South Korea

*Corresponding author: Fax: +82 41 6883352; E-mail: wc_oh@hanseo.ac.kr

(*Received*: 4 January 2011; *Accepted*: 24 September 2011) AJC-10438

Reduced graphene-based sheets were produced by reduction of a colloidal suspension of expanded graphite oxide sheets in water with hydrazine hydrate. These sheets were comprehensively characterized by Fourier transform infrared spectroscopy, energy dispersive X-ray analysis, X-ray diffraction, scanning electron microscopy, transmission electron microscopy and Raman spectroscopy. X-ray diffraction, energy dispersive X-ray and Fourier transform infrared measurements indicate the formation of strong functional groups of expanded graphite oxide. From the transmission electron microscopy images, graphene based nanosheets could be found in the reduction of expanded graphite oxide. The Raman spectra indicated that the stacking structure and agglomerated morphology of graphene based nanosheets is deduced.

Key Words: Graphene, Expanded graphite, Nano sheet.

INTRODUCTION

Atomically thick graphene layers produced from graphite reveal unique electro-thermal and mechanical properties[1-7] and are considered to have a wide range of applications in nanoelectronics[1], catalysis[2] and biosensing[8-11]. These excellent properties may be relevant at the nanoscale if graphite can be exfoliated into thin nanosheets and even down to the single graphene sheet level[12]. Graphene monolayers have been prepared by mechanical exfoliation[1,2], epitaxial growth[13] or *via* thermal fusion[14]. However these methods are constrained by low yields and processing limitations.

Expanded graphite (EG) is a kind of modified and low-density graphite with a good surface area, electrical conductivity and high temperature resistance[15]. When graphite intercalation compounds (GICs) are given a thermal shock, the intercalates vapourize and tear the layers apart that leads to an expansion in the c direction and in a puffed-up material. Expanded graphite contains abundant multi-pores ranging from 20 to 50 nm. The interlayer spacing of expanded graphite increases from 0.335 nm to *ca.* 0.8 nm and that of expanded graphite are several hundred times along the c-axis[16,17]. Expanded graphite is used to sorption the polluted oil and various kinds of polluted gas. It has been also applied widely as a kind of functional carbon material used in sealing, catalyzing, space flight, military affairs, environmental protection, *etc.*[18,19]. The expanded graphite keeps a layered structure similar to natural graphite flakes but with larger interlayer spacing.

Our interest in the preparation of graphene-based materials, we set out to develop a general and reproducible approach for the preparation of graphene sheets from expanded graphite. Graphite nanosheets have often been made from expanded graphite, which in turn was produced from graphite intercalation compounds *via* rapid evaporation of the intercalant at elevated temperatures. Although this simple method has been applied on a large scale to commercially available sulfuric acid intercalated graphite, it never results in complete exfoliation of graphite to the level of individual graphene sheets. Herein, we decided to use expanded graphite oxide (EGO) as one possible route for meeting this challenge. Our basic strategy involved the complete exfoliation of expanded graphite oxide into individual expanded graphite oxide sheets followed by their *in situ* reduction to produce individual graphene-like sheets. We describe the detailed process for the reduction of expanded graphite oxide sheets with hydrazine and the characterization of the resulting material.

EXPERIMENTAL

Preparation of expanded graphite: Expanded graphite was prepared from natural graphite (NG). Natural graphite

with an 80-100 mesh size was obtained from SangJin Co., Ltd., Korea. Graphite intercalation compounds (GICs) yielding expanded graphite upon a thermal shock were obtained using chemical oxidation intercalation. At first, 3 g of $(NH_4)_2SO_4$ was melted in 100 mL H_2SO_4. Then 1 g natural graphite was put into $(NH_4)_2SO_4$-H_2SO_4 solution and stirring at 323 K for 0.5 h. The mixture was carefully washed and filtrated with distilled water until the pH level of solution reached 7. After being dried at 373 K for 24 h, the graphite intercalation compunds were rapidly expanded at 873 K for 1 h to form expanded graphite.

Preparation of expanded graphite oxide: Expanded graphite oxide was prepared from expanded graphite according to the Hummers-Offeman method[20]. In brief, expanded graphite powder (2 g) was dispersed in cold concentrated sulphuric acid (46 mL, 98 wt %, dry ice bath) and potassium permanganate ($KMnO_4$, 6 g) gradually added with continuous vigorous stirring and cooling to prevent the temperature from exceeding 293 K. The dry ice bath was removed and replaced by a water bath and the mixture heated to 308 K for 0.5 h with gas release under continuous stirring, followed by slow addition of deionized water (92 mL), which produced a rapid increase in solution temperature up to a maximum of 371 K. The reaction was maintained for 40 min in order to increase the oxidation degree of the expanded graphite oxide product and then the resultant bright-yellow suspension was terminated by addition of more distilled water (140 mL) followed by hydrogen peroxide solution (H_2O_2, 30 %, 30 mL). The solid product was separated by centrifugation at 3000 rpm and washed initially with 5 % HCl until SO_4^{2-} were no longer detectable with barium chloride and then washed three times with acetone and air dried overnight at 338 K.

Reduction of expanded graphite oxide: Reduction of expanded graphite oxide was performed as follows: 25 mg of the expanded graphite oxide powder was placed in a cup and 200 mL de-ionized water was then added. Ten min of magnetic stirring at 200 rpm yielded an inhomogeneous brown suspension. The resulting suspensions were further treated with a reduction agent hydrazine solution (1:5, volume ratio of hydrazine to de-ionized water) under ultrasonication (0.5 h, 1.3×10^5 J) and after dried at 373 K, the sample of reduction of expanded graphite oxide was produced.

Characterizations of samples: XRD measurements were performed for expanded graphite, expanded graphite oxide and reduced expanded graphite oxide samples at room temperature. XRD patterns were obtained with a diffractometer (Shimata XD-D1, Japan) using CuK_α radiation. SEM was used to observe the surface state and structure of the samples using a scanning electron microscope (JOEL, JSM-5200, Japan). EDX spectroscopy was used to measure the elemental analysis of the composites. Raman spectra were utilized to detect the possible structural defects in graphene flakes. The measurements were carried out by a Horiba Jobin Yvon LabRAM using a 100 × objective lens with a 532 nm laser excitation. Thin films (*ca.* 30 nm) were prepared by vacuum filtration of the dispersions through porous alumina membranes. The state of the dispersed graphene was observed using transmission electron microscopy (TEM, JEOL, JEM-2010, Japan). TEM at an acceleration voltage of 200 kV was used to investigate the number and the stacking state of graphene-based nanosheets on various samples. TEM specimens were prepared by placing a few drops of sample solution on a carbon grid. Fourier transform-infrared (FT-IR) spectroscopy (FTS 3000MX, Biored Co.) was used to characterize the composite materials.

RESULTS AND DISCUSSION

The results of the EDX elemental microanalysis of C and O elements are listed in Table-1. The C contents of the expanded graphite, expanded graphite oxide and reduced expanded graphite oxide are 83.49, 48.98 and 71.79 %, respectively. It can be expected that the C contents of the reduced expanded graphite oxide in the composites increased due to reduction treatment of partial oxygen containing functional groups. Moreover, the O contents of reduced expanded graphite oxide are only 13.15 % and the mass ratio of O/C is 0.18. It was indicated that some oxygen containing functional groups were still existed in the sample of reduced expanded graphite oxide. Moreover, the mass ratio of O/C for reduced expanded graphite oxide decreased to about 0.25 of that of expanded graphite oxide. It was noted that the increase in nitrogen contents after reduction most likely originated from the reactions between expanded graphite oxide and the reducing agent[21-23]. Hydrazine readily reacted with the epoxide functional groups to form hydrazine alcohols, which were mainly responsible for the incorporation of nitrogen.

TABLE-1
EDX ELEMENTAL MICROANALYSIS OF C, O AND N ELEMENTS

Samples	Elements (wt.%)			
	C	O	N	O/C ratio
EG	83.49	8.60	–	0.10
EGO	48.98	44.76	–	0.91
REGO	71.79	13.15	5.42	0.18

EG = Expanded graphite, EGO = Expanded graphite oxide, REGO = Reduced expanded graphite oxide

The chemical changes occurring upon the treatment of graphite oxide with organic diisocyanates can be observed by IR spectroscopy. The IR spectra of powdery expanded graphite, expanded graphite oxide and reduced expanded graphite oxide are shown in Fig. 1. The spectrum of the powdery expanded graphite oxide shows characteristic absorption bands corresponding to the C=O carbonyl stretching at 1723 cm^{-1}, the C-OH stretching at 1244 cm^{-1} and the C-O stretching at 1393 cm^{-1}. The resonance at 1622 cm^{-1} is assigned to the vibrations of the aromatic C=C, but may also contain components from the skeletal vibrations of un-oxidized graphitic domains. The peaks of reduced expanded graphite oxide for functional groups were reduced after chemical reduction. Combination with the EDX analysis and the peaks change of FT-IR, it is considered that there were still certain of oxygen existing in the sample of reduced expanded graphite oxide. But the mass ratio of O/C is 0.18, which is very near to the pristine value (0.10, for the expanded graphite case). It was indicated that a successful formation of graphene based materials has been completed. Nevertheless, two weak, but sharp peaks turned

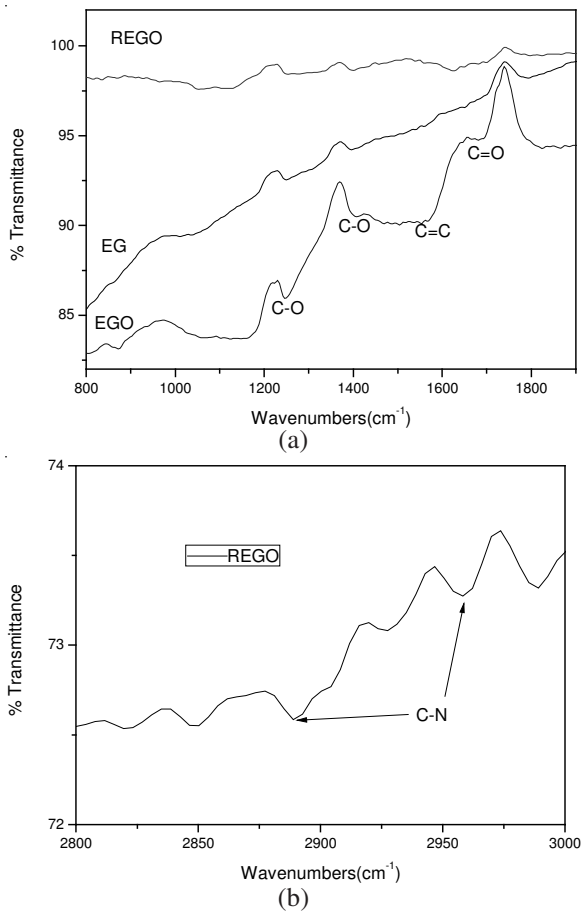

Fig. 1. FTIR spectra of EG, EGO and REGO (a) and the magnified C-N stretch vibration in the spectrum of REGO (b)

up within the range of 2960-2850 cm^{-1} corresponding to C-N stretch vibration was found in the Fig 1(b), which is consistent with the EDX analysis (Table-1).

XRD patterns of powdery expanded graphite, expanded graphite oxide and reduced expanded graphite oxide are presented in Fig. 2. There are different assignments of the peaks for different samples. The XRD pattern of expanded graphite sample contained a very sharp and high intensity 002 peak near $2\theta = 26.5°$ and 004 peak near $2\theta = 54.5°$ (Fig. 2(a)). Due to oxidation, the crystal nature of the expanded graphite oxide was changed and occurrence of a broad 001 peak near $2\theta = 13.5°$ and a relatively wider and very low intensity 002 peak near $2\theta = 27.5°$ were observed in the XRD pattern of expanded graphite oxide (Fig. 2(b)), due to the existence of oxygen-rich groups on both sides of the sheets and water molecules trapped between the sheets[24,25]. Chemical reduction restored the crystal structure again in graphene based nanosheets (REGO) by removing the effect of oxidation observed in the expanded graphite oxide sample; a sharp and high intensity 002 peak near $2\theta = 26.5°$ was observed in the XRD pattern of the reduced expanded graphite oxide (Fig. 2(c)), which may be due to a modification of graphene sheets by chemical reduction treatment.

The morphology of our "as prepared" powder sample was examined by SEM and TEM; representative images are shown in Figs. 3 and 4, respectively. Fig. 3 shows the SEM images of expanded graphite, expanded graphite oxide and reduced expanded graphite oxide, respectively. The sample expanded

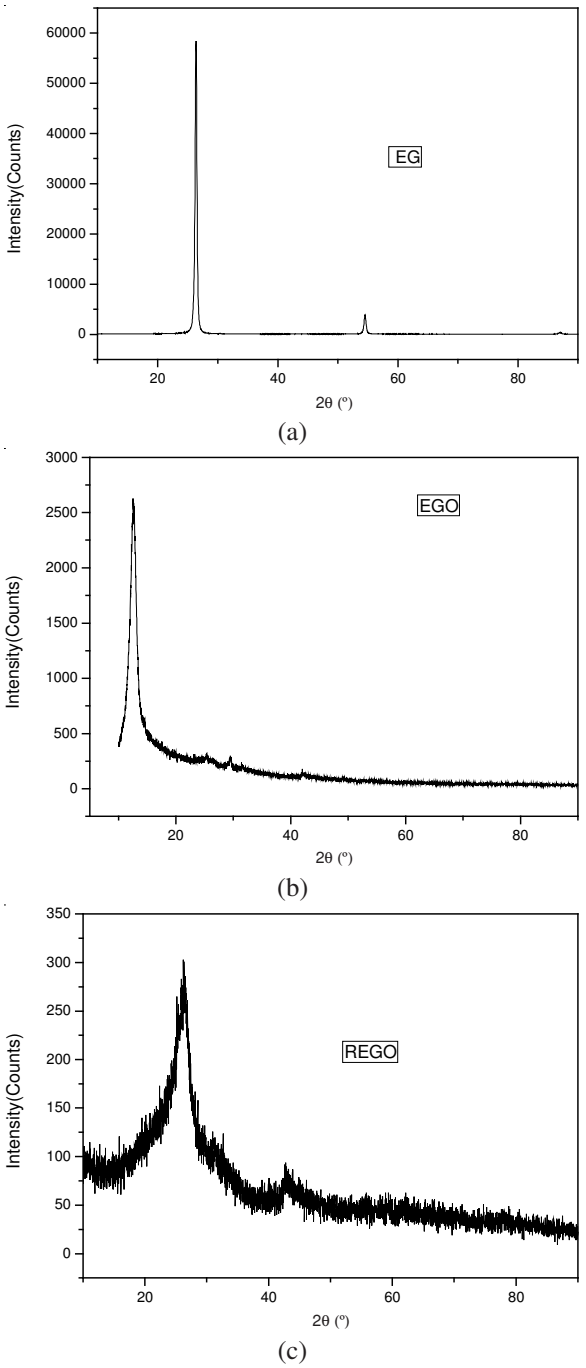

Fig. 2. XRD patterns of EG (a), EGO (b) and REGO (c)

graphite shows flaky like forms with rigid and compacted layers. After oxidation reactions, the morphology of expanded graphite oxide was also investigated by SEM and the graphite oxide sheets become swollen [Fig. 3(b)]. It appeared that higher sulfuric acid amount increased the effect of oxidation caused by the dichromate ions. With this amplified effect of oxidation, it was possible that more oxygen atoms were force to attach to graphite layers which resulted in a more loose structure compared to that of the rigid structure of raw graphite. The oxidation step depends on the amount of sulfuric acid used in this reaction. Heat treatment of such treated samples led to the thermal decomposition of acetic anhydride into CO_2 and H_2O vapour which further swelled the layered graphitic structure. The heat treatment process caused the expansion of graphitic

crystal lattice and further separated the tulle-like graphite oxide sheets. The tulle-like graphene based sheets were even more easily observable in the SEM images of the reduced expanded graphite oxide samples and the layers became wavy, Fig. 3(c). This might have stemmed from the effect of ultrasonication treatment period that could not initiate the separation of the graphene based sheets. The TEM (Fig. 4) image shows a wrinkled and disordered graphene sheet-like structure. It is known that the synthesis of graphene materials from reduction of expanded graphite oxide generally yields samples which are not based on single separated graphene sheets, but rather on an inter-connected network with regions of over-lapped multiple layers[21]. This process also yields a highly agglomerated wrinkled sheet structure, resulting primarily from the high compliance of such extremely thin platelets, with a possible further contribution from reaction sites involved in oxidation and reduction processes[21].

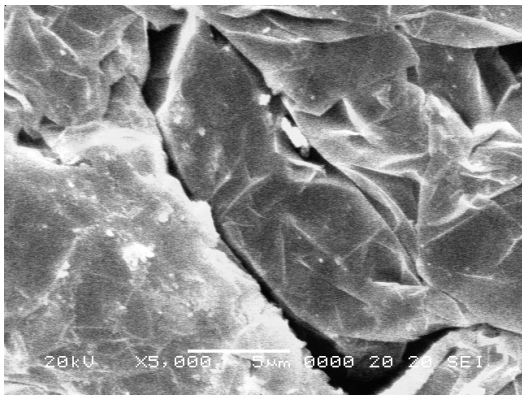

(a)

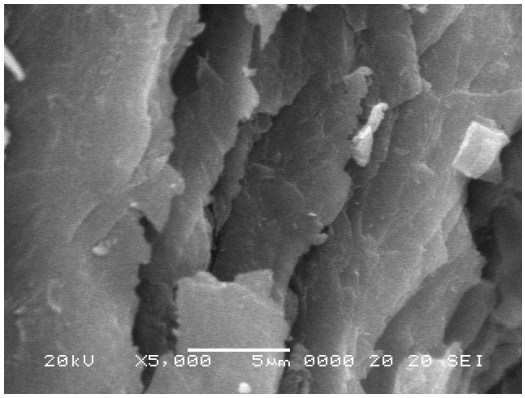

(b)

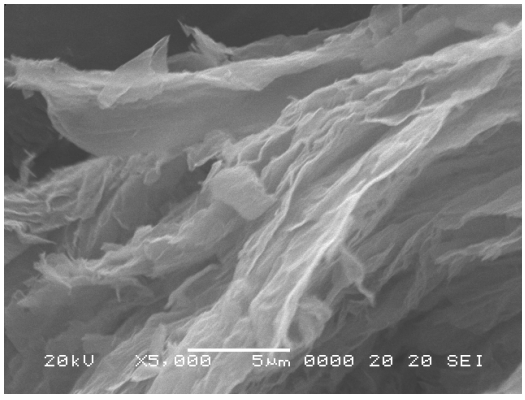

(c)

Fig. 3. SEM images of EG (a), EGO (b) and REGO (c)

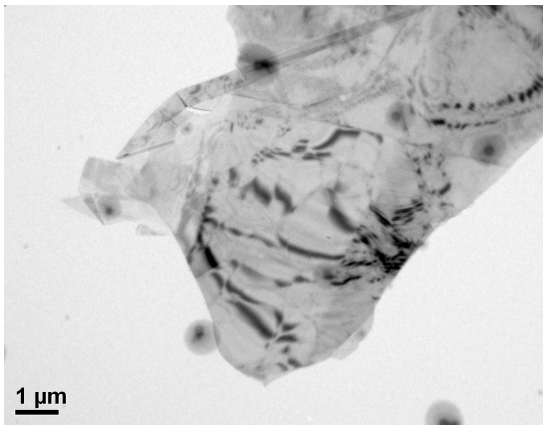

(a)

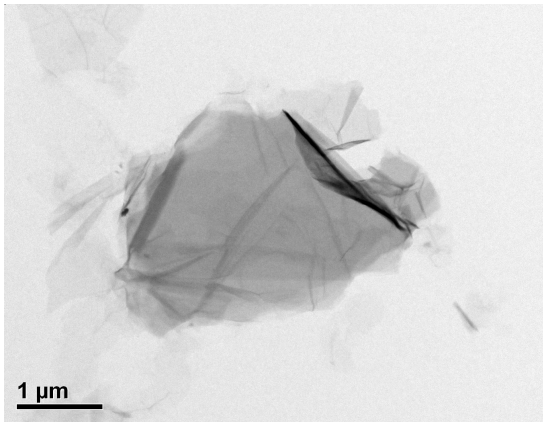

(b)

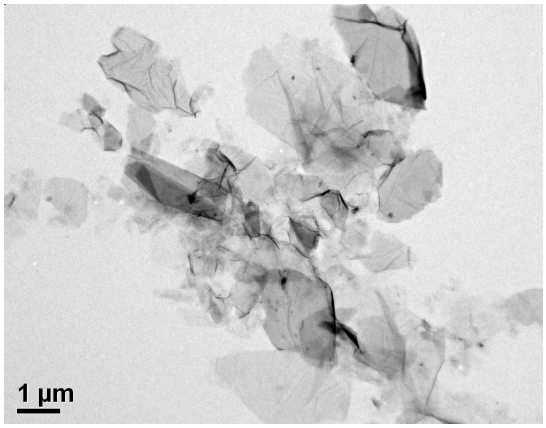

(c)

Fig. 4. TEM images of EG (a), EGO (b) and REGO (c)

Raman spectroscopy is a quick and accurate technique to determine the number of graphene layers and the change of crystal structure of the materials after chemical treatments[26]. There are four remarkable peaks in the Raman spectrum of graphite which are the G band around 1580 cm^{-1}, the 2G band (the overtone of the G band) around 3248 cm^{-1}, the D band around 1360 cm^{-1} and the 2D band (the overtone of the D band) around 2700 cm^{-1}. The intensity of the D band depends on the amount of the disorderness of the graphitic materials and its position shifts regarding to incident laser excitation energies[26].

Fig. 5 shows the Raman spectrum of the powdery expanded graphite, expanded graphite oxide and reduced expanded

graphite oxide. A sharp G band at 1580 cm^{-1}, a weak D band at 1356 cm^{-1} and a strong 2D line at 2725 cm^{-1} were seen in the Raman spectrum of expanded graphite sample [Fig. 5(a)]. After oxidation process, G band of expanded graphite oxide sample was broadened and the intensity of D band was increased due to the reduction in the thickness of the graphitic structure [Fig. 5(b)]. In the Raman spectrum of reduced expanded graphite oxide, the G band was broadened and shifted to 1589 cm^{-1} [Fig. 5(c)]. In addition, an increased intensity of the D band around 1353 cm^{-1} indicated the considerable reduction in size of the in-plane sp^2 domains owing to oxidation process and the formation of graphene based nanosheets having highly oriented crystal structure. In the Raman spectrum of graphene based nanosheets obtained after chemical reduction of expanded graphite oxide, the intensity of the D band around 1353 cm^{-1} decreased considerably as a result of an increase of the graphitic domain sizes and an increase of the thickness of graphitic structure after thermal treatment. Moreover, the D bands of expanded graphite oxide and reduced expanded graphite oxide are relatively intense compared to the G band, which is in agreement with previous results for graphene samples obtained from exfoliated graphite oxide[27].

It was shown that along the expanded graphite-reduced expanded graphite oxide-expanded graphite oxide path the Raman spectra undergo significant changes. Specifically, the G band broadened significantly and displayed a shift to higher

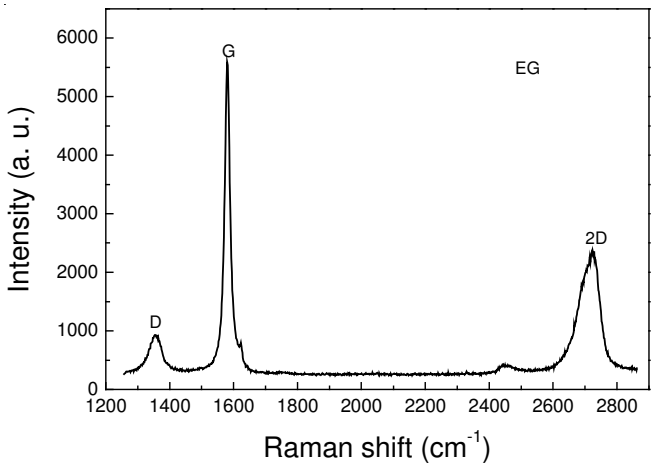

(a)

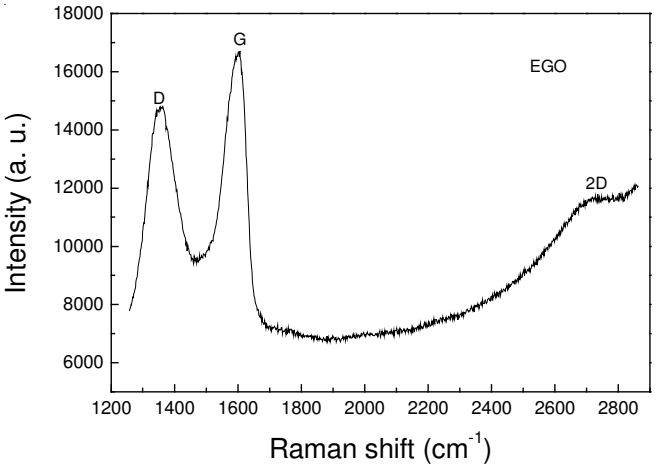

(b)

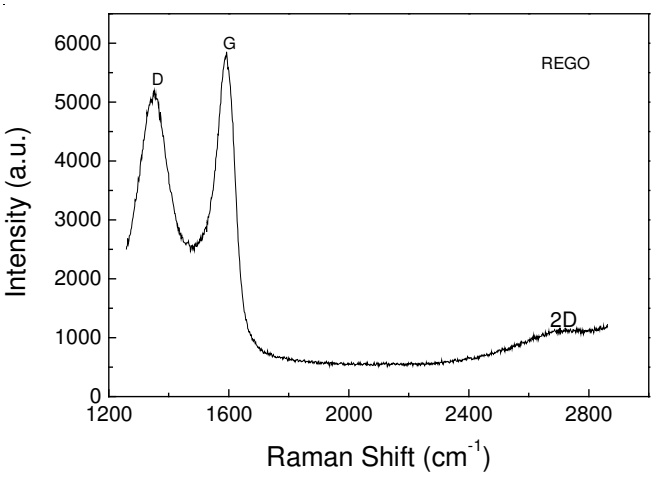

(c)

Fig. 5. Raman spectra of EG (a), EGO (b) and REGO (c)

frequencies (blue-shift) and the D band grew in intensity. This shift was also observed when going from a graphite crystal to a single graphene sheet, in which the G band shifts to a value 3-6 cm^{-1} higher than for bulk graphite[28,29]. And the shift of the G band and relatively intense D band indicate small stacks of quite disordered graphene sheets. The ratio of the G band to D band intensity can be related to the in-plane crystallite size[30]. The second-order Raman feature, namely the 2D band (second-order of the D band) at about 2720 cm^{-1}, is very sensitive to the stacking order of the graphene sheets along the c-axis as well as to the number of layers and shows greater structure (often a doublet) with increasing number of graphene layers. The stacking structure and agglomerated morphology of the reduced graphene sheets is therefore consistent with as deduced from our XRD and TEM studies.

Conclusion

In this study, graphene based nanosheets were produced *via* the chemical reduction of expanded graphite oxide. FT-IR spectroscopy showed that the peaks for functional groups were reduced after chemical reduction, indicating a successful formation of graphene based materials. The tulle-like graphene based sheets were more easily observable for the reduced expanded graphite oxide samples in the SEM images and the TEM image also shows a wrinkled and disordered graphene sheet-like structure. The Raman spectrum of reduced expanded graphite oxide showed that the G band broadened significantly and displayed a shift to higher frequencies (blue-shift) and the D band grew in intensity.

REFERENCES

1. K.S. Novoselov, A.K. Geim, S.V. Morozov, D. Jiang, Y. Zhang, S.V. Dubonos, I.V. Grigorieva and A.A. Firsov, *Science*, **306**, 666 (2004).
2. K.S. Novoselov, A.K. Geim, S.V. Morozov, D. Jiang, M.I. Katsnelson, I.V. Grigorieva, S.V. Dubonos and A.A. Firsov, *Nature*, **438**, 197 (2005).
3. J.C. Meyer, A.K. Geim, M.I. Katsnelson, K.S. Novoselov, T.J. Booth and S. Roth, *Nature*, **446**, 60 (2007).
4. A.K. Geim and K.S. Novoselov, *Nature Mater.*, **6**, 183 (2007).
5. Y. Zhang, Y.-W. Tan, H.L. Stormer and P. Kim, *Nature*, **438**, 201 (2005).
6. S. Stankovich, D.A. Dikin, G.H.B. Dommett, K.K. Kohlhaas, E.J. Zimney, E.A. Stach, R.D. Piner, S.T. Nguyen and R.S. Ruoff, *Nature*, **442**, 282 (2006).

7. T. Ramanathan, A.A. Abdala, S. Stankovich, D.A. Dikin, M. Herrera-Alonso, R.D. Piner, D.H. Adamson, H.C. Schniepp, X. Chen, R.S. Ruoff, S.T. Nguyen, I.A. Aksay, R.K. Prud'homme and L.C. Brinson, *Nat. Nanotechnol.*, **3**, 327 (2008).
8. N.A. Kotov, I. Dekany and J.H. Fendler, *Adv. Mater.*, **8**, 637 (1996).
9. G. Eda, G. Fanchini and M. Chhowalla, *Nat. Nanotechnol.*, **3**, 270 (2008).
10. N. Mohanty and V. Berry, *Nano Lett.*, **8**, 4469 (2008).
11. A.J. Patil, J.L. Vickery, T.B. Scott and S. Mann, *Adv. Mater.*, **21**, 1 (2009).
12. N.A. Kotov, *Nature*, **442**, 254 (2006).
13. C. Berger, Z.M. Song, X.B. Li, X.S. Wu, N. Brown, C. Naud, D. Mayo, T.B. Li, J. Hass, A.N. Marchenkov, E.H. Conrad, P.N. First and W.A. de Heer, *Science*, **312**, 1191 (2006).
14. X. Wang, L. Zhi, N. Tsao, Z. Tomovic, J. Li and K. Mullen, *Angew. Chem. Int. Ed.*, **47**, 2990 (2008).
15. D.D.L. Chung, *J. Mater. Sci.*, **22**, 4190 (1987).
16. F. Kang, T.Y. Zhang and Y. Leng, *Carbon*, **35**, 1167 (1997).
17. G.H. Chen, D.J. Wu, W.C. Weng, B. He and W.L.Yan, *Polym. Int.*, **50**, 980 (2001).
18. M. Toyada and M. Inagaki, *Carbon*, **38**, 199 (2000).
19. A. Celzard, J.F. Mareche, G. Furdin and S. Puricelli, *J. Phys. D Appl. Phys.*, **33**, 3094 (2000).
20. W.S. Hummers and R.E. Offeman, *J. Am. Chem. Soc.*, **80**, 1339 (1958).
21. S. Stankovich, D.A. Dikin, R.D. Piner, K.A. Kohlhaas, A. Kleinhammes, Y. Jia, Y. Wu, S.T. Nguyen and R.S. Ruoff, *Carbon*, **45**, 1558 (2007).
22. H.C. Schniepp, J. Li, M.J. Mcallister, H. Sai, M. Herrera-Alonso, D.H. Adamson, R.K. Prud'homme, R. Car, D.A. Saville and I.A. Aksay, *J. Phys. Chem. B*, **110**, 8535 (2006).
23. Y. Geng, S.J. Wang and J.K. Kim, *J. Colloid. Interf. Sci.*, **336**, 592 (2009).
24. G.I. Titelman, V. Gelman, S. Bron, R.L. Khalfin and Y. Cohen, *Carbon*, **43**, 641 (2005).
25. M. Mermoux, Y. Chabre and A. Rousseau, *Carbon*, **29**, 469 (1991).
26. D. Graf, F. Molitor, K. Ensslin, C. Stampfer, A. Jungen and C. Hierold, *Nano. Lett.*, **7**, 238 (2007).
27. K.S. Subrahmanyam, S.R.C. Vivekchand, A. Govindaraj and C.N.R. Rao, *J. Mater. Chem.*, **18**, 1517 (2008).
28. A.C. Ferrari, J.C. Meyer, V. Scardaci, C. Casiraghi, M. Lazzeri, F. Mauri, S. Piscanec, D. Jiang, K.S. Novoselov, S. Roth and A.K. Geim, *Phys. Rev. Lett.*, **97**, 187401 (2006).
29. A. Gupta, G. Chen, P. Joshi, S. Tadigadapa and P.C. Eklund, *Nano. Lett.*, **6**, 2667 (2006).
30. M.A. Pimenta, G. Dresselhaus, M.S. Dresselhaus, L.A. Cancado, A. Jorio and R. Sato, *Phys. Chem. Chem. Phys.*, **9**, 1276 (2007).